

Progress Report #1:  
Radio Frequency Noise Reduction in the LIGO Hanford  
Observatory

Matthew O. Withers  
*Department of Physics and Engineering*  
*Washington and Lee University*

Mentor: Dick Gustafson  
Co-Mentor: Keita Kawabe

July 10, 2019

# Elimination of Non-Linear Harmonics in LHO's RF Generation System

Prior to the start of this project, LIGO technicians had reported numerous non-linearities in the outputs of LHO's RF signal generation system. These non-linearities usually appear as a comb of harmonics above the RF carrier frequency. Since the RF signal generation system provides the RF signal necessary to control the IFO's control drivers, ensuring that these signals are free of any unintended harmonics is important to increasing the duty factor of the observatory.

I began my search for these reported harmonic combs by measuring the power spectra of disused outputs on the various LIGO RF Distribution Amplifiers (D1000124) currently installed in LHO's CER and LVEA. These measurements revealed that every amplifier exhibited the reported comb structure. Table 1 summarizes the harmonics present in the output of an RF Distribution Amplifier receiving an 80 MHz RF signal (10 dBm) from a standard LIGO RF Oscillator Source (D080702).<sup>1</sup>

Table 1: The strength of various harmonics produced by an RF Distribution Amplifier accepting an 80 MHz RF signal, as measured by an Agilent 9396B Spectrum Analyzer.

Frequency (MHz)	Strength Relative to Carrier (dBc)
80 (Carrier Frequency)	0
160	-24.8
240	-26.4
320	-33.3
400	-36.1
480	-38.1

Values such as these are typical for the RF Distribution Amplifiers currently in use at LHO.

To ensure the purity of the observatory's RF signals, we sought to improve the output reducing the harmonic dBc values to at most -60 dB. Achieving this goal required further analysis of the RF signal generation system in isolation from the rest of the IFO. To achieve this isolation, I acquired a spare RF Oscillator Source (10 MHz) and installed it in the LHO electrical engineering laboratory. I also constructed an RF Distribution Amplifier using plans available on the DCC (D1000124) since no spare units were available. With this isolated system constructed, I first considered whether the harmonics were being produced by the oscillator or the amplifier by examining the output of each unit individually. Figure 1 gives the output of the RF Oscillator Source when measured with a spectrum analyzer, while Table 2 summarizes the dBc of each peak present.

---

<sup>1</sup>The RF Oscillator Source under consideration can be found at ISC-C3-25, while the RF Distribution Amplifier can be found at ISC-C3-23.

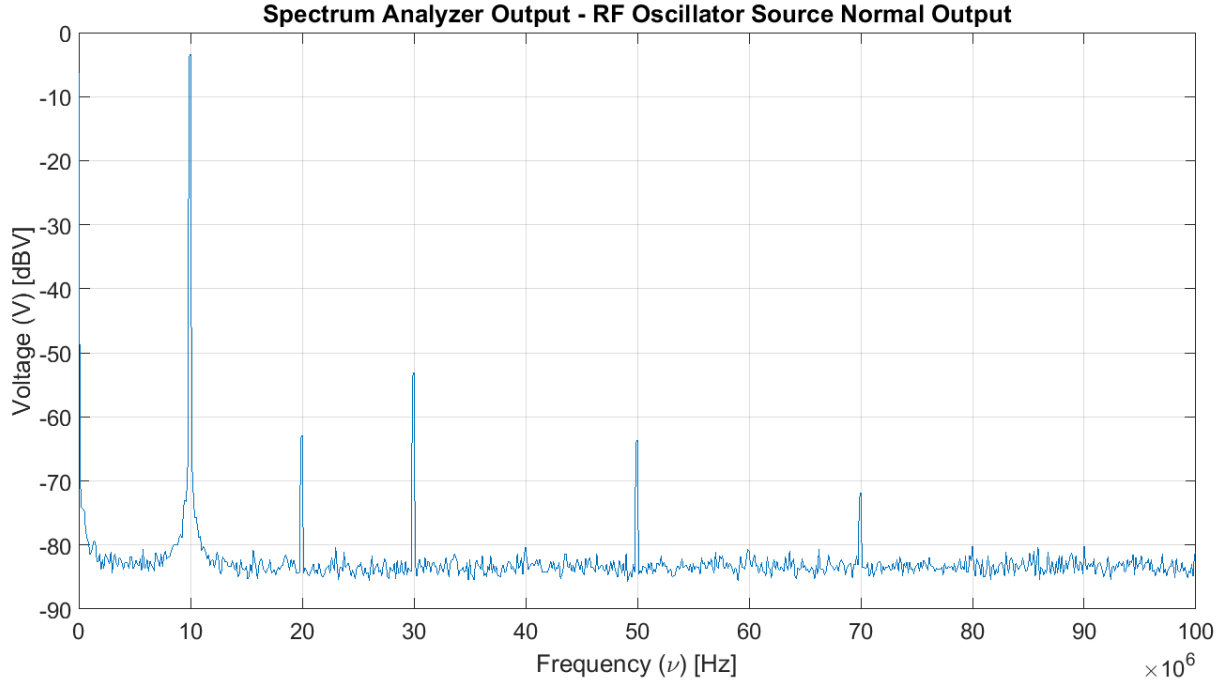


Figure 1: The spectrum analyzer output of my isolated 10 MHz RF Oscillator Source. Notice the presence of noise at 10, 30, 50, and 70 MHz.

Table 2: The strength of various harmonics produced by an isolated 10 MHz RF Signal Generator.

Frequency (MHz)	Strength Relative to Carrier (dBc)
10 (Carrier Frequency)	0
20	-59.43
30	-49.68
50	-60.27
70	-68.38

This output clearly demonstrates that a small amount of the RF system’s harmonic noise arises within the oscillator unit. Because proper testing of the RF Distribution Amplifier requires a clean signal from the oscillator, I sought to eliminate these harmonics before continuing my investigation. The simplest solution to noise above the carrier frequency is to insert a low-pass filter with a cutoff (-3 dB) frequency that is slightly higher than the carrier frequency. Figure 2 shows the spectral analyzer readout of the RF Oscillator Source with a Mini Circuits 15-SLP filter installed just before the output. The figure clearly demonstrates that the installation of a low-pass filter successfully eliminates all of the harmonics produced by the oscillator. Furthermore, the filter’s installation has no effect on the output voltage of the carrier.

With the noise produced by the RF Oscillator Source eliminated, I then turned my attention to the RF Distribution Amplifier. Figure 3 shows the spectrum analyzer reading of the amplifier when it receives a signal from the (now filtered) 10 MHz RF Oscillator Source, while Table 3 gives the strength of each harmonic relative to the carrier frequency.

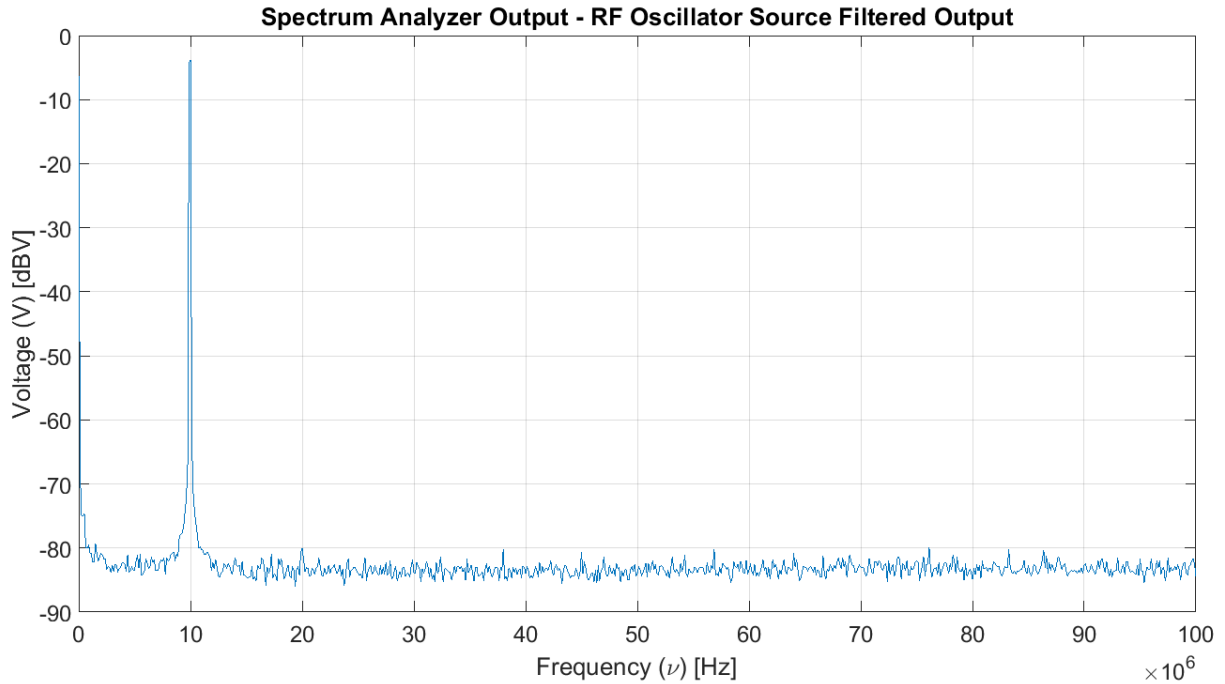


Figure 2: The spectrum analyzer readout of my isolated 10 MHz RF Oscillator Source when filtered with a Mini Circuits 15-SLP low-pass filter. Notice the lack of harmonic frequencies, indicating a pure oscillator signal.

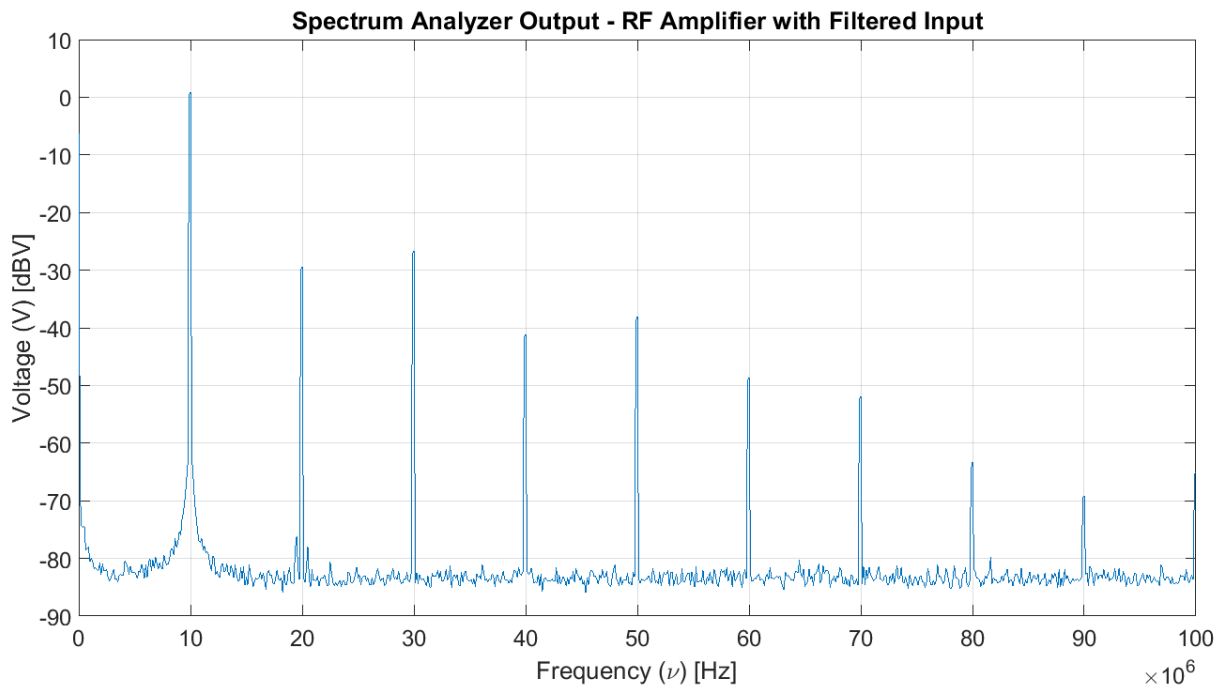


Figure 3: The spectrum analyzer readout of my isolated RF Distribution Amplifier when it receives an RF signal from an appropriately filtered 10 MHz RF Oscillator Source. Notice the strong harmonics above the carrier, providing almost all of the comb structure observed by physicists and engineers servicing LHO's RF signal generation system.

Table 3: The strength of various harmonics produced by my isolated RF Distribution Amplifier when it receives an RF signal from an appropriately filtered 10 MHz RF Oscillator Source.

Frequency (MHz)	Strength Relative to Carrier (dBc)
10 (Carrier Frequency)	0
20	-28.46
30	-25.64
40	-40.70
50	-37.70
60	-48.20
70	-50.88
80	-62.32
90	-68.16

These data indicate that the RF Distribution Amplifier provides the majority of the noise extant in the harmonic comb. My next course of action was to identify the specific electrical component contained within the amplifier unit responsible for producing the harmonics. Figure 4 shows the schematic of the amplifier's internal components. I initially hypothesized that the harmonics were being produced by U1, the unit's single RF amplifier, because it is the only active component acting on the input RF signal. To test this theory, I disconnected U1 from the RF coupler (U2) and measured its output directly using the spectrum analyzer. Once again, I used the filtered RF signal produced by the 10 MHz RF Signal Generator as the input. The resulting analyzer output was almost identical to the one contained in Figure 3. Because there are no components in the amplifier unit prior to U1, this result was sufficient to indicate that U1 was the source of the harmonics.

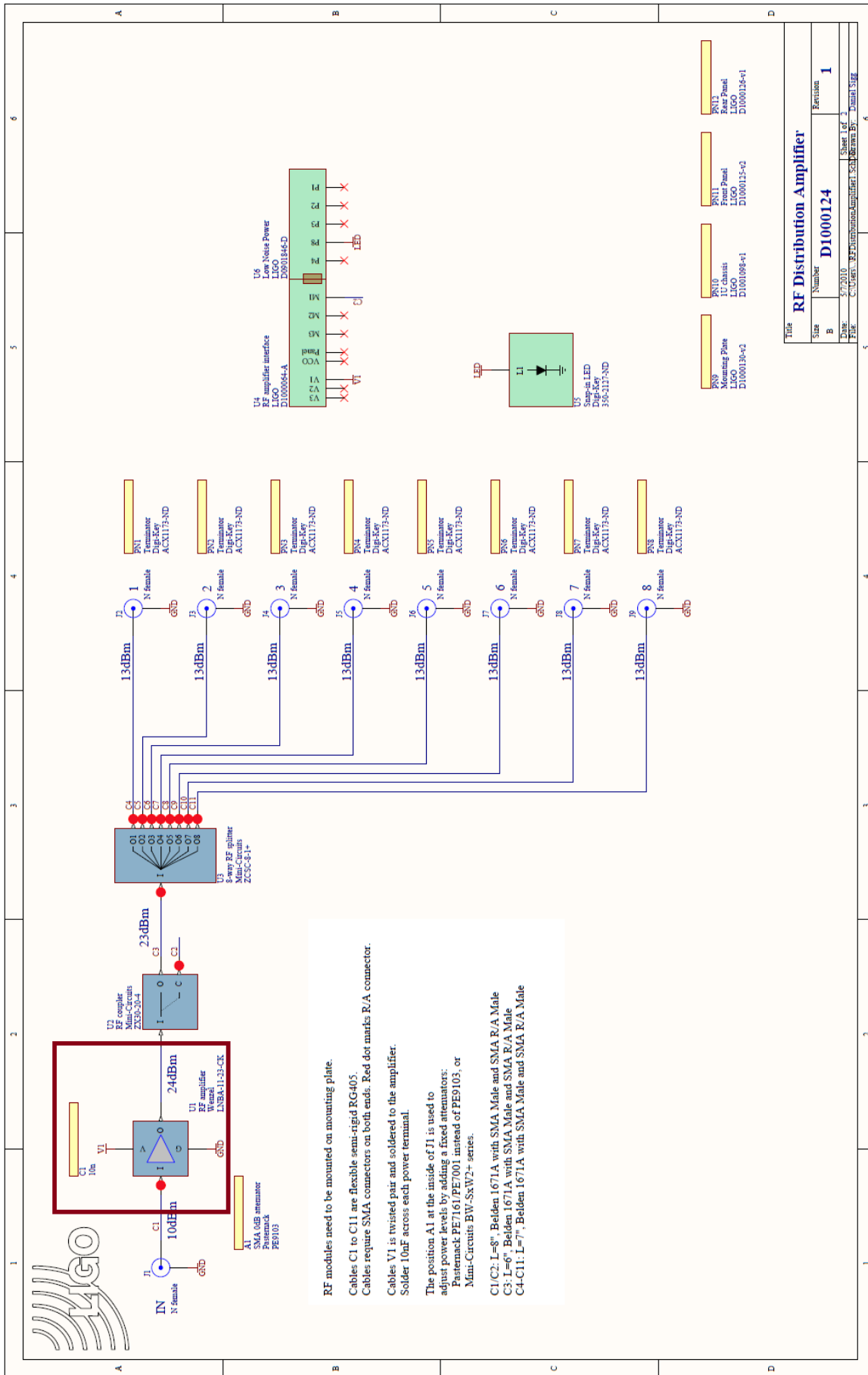


Figure 4: A schematic of the internal components of an RF Distribution Amplifier, found as D1000124 on the DCC. My investigation identified component U1 (see the red box), an RF amplifier, as the source of the harmonic noise present at the output of the module.

After identifying U1 as the source of the harmonics, I consulted its data sheet [1] to determine whether it was behaving according to its manufacturer-determined specifications. The data sheet suggests that all Wenzel LNBA RF amplifiers should produce harmonics that are less than or equal to 25 dBc. Because the RF signal generation system requires a dBc of -60 or more, such an amplifier cannot suppress these harmonics to the necessary level as designed. An extensive search for alternative RF amplifiers revealed that most, if not all, amplifiers on the market have a similar harmonic tolerance. Thus, the most cost effective solution to the harmonics problem seemed to be the inclusion of an appropriately selected low-pass filter between U1 and U2. Figure 5 shows the spectrum analyzer output for my test RF Distribution Amplifier with an SLP-10.7 low-pass filter included at this location. Additionally, Table 4 details the strength of the remaining harmonics.

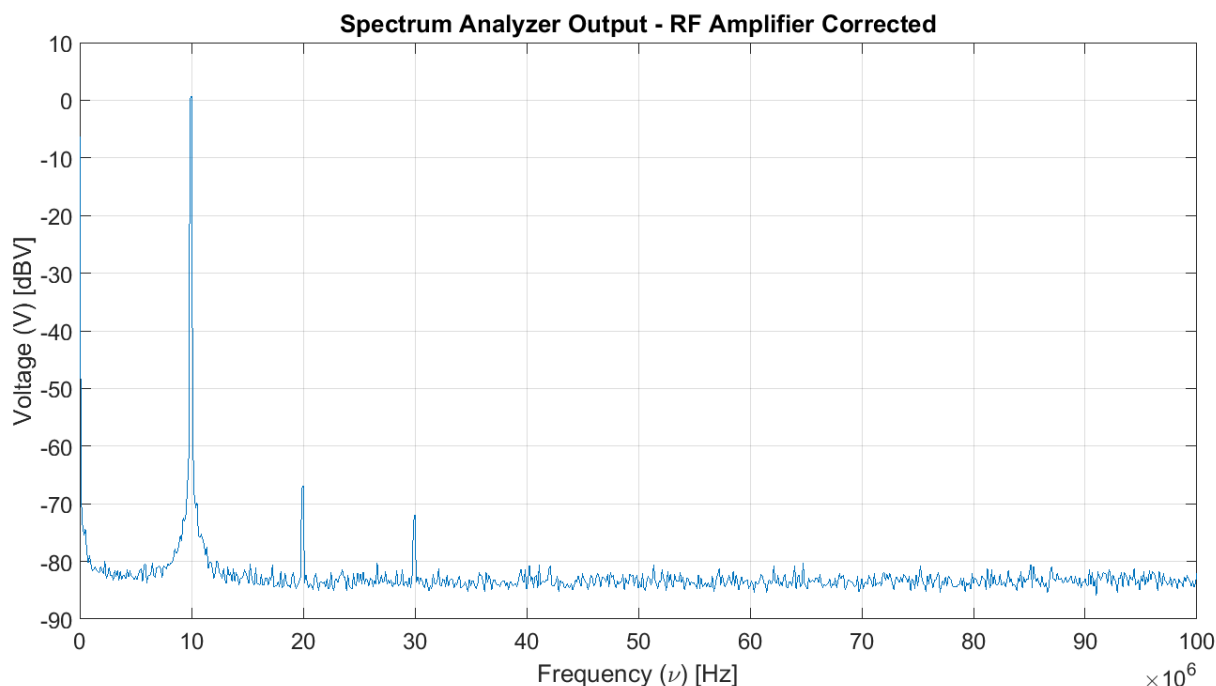


Figure 5: The spectrum analyzer readout of my isolated RF Distribution Amplifier when an SLP-10.7 low-pass filter is included between U1 and U2. Notice the near elimination of the harmonics present in Figure 3.

Table 4: The strength of various harmonics produced by an isolated 10 MHz RF Signal Generator.

Frequency (MHz)	Strength Relative to Carrier (dBc)
10 (Carrier Frequency)	0
20	-67.50
30	-72.67

Clearly, the inclusion of the low-pass filter eliminates nearly all of the harmonics. Those that remain are well below the desired -60 dBc.

The final aspect of this problem is determining the filters necessary to correct the output of every RF Signal Generator and RF Distribution Amplifier currently in use at LHO. Each

filter must be selected to allow the carrier frequency to sit comfortably within the pass band while the harmonics fall well within the attenuation band (preferably past the -40 dB cutoff). Table 5 lists each unit requiring a filter, its location, its carrier frequency, its first harmonic, the selected filter, and the filter’s maximum passband frequency and -40 dB cutoff.

Table 5: A summary of the RF Distribution Amplifiers and RF Oscillator Sources currently in use at LHO, accompanied by the filter needed to correct their respective harmonic combs.

<b>Unit Type</b>	<b>Location</b>	<b>Carrier Frequency (MHz)</b>	<b>First Harmonic (MHz)</b>	<b>Selected Filter (MHz)</b>	<b>Passband Cutoff (MHz)</b>	<b>-40 dB Cutoff (MHz)</b>
Dist. Amp.	ISC-R1-36	70.625	141.25	SLP-90+	81	121
Dist. Amp.	ISC-R1-35	24	48	SLP-30+	32	47
Dist. Amp.	ISC-R2-38	45.3	90.6	SLP-50+	48	70
Dist. Amp.	ISC-R2-37	9.1	18.2	SLP-10.7+	11	19
Dist. Amp.	ISC-C3-23	80	160	SLP-90+	81	121
Dist. Amp.	ISC-C3-27	35	70	SLP-50+	48	70
Dist. Amp.	ISC-C3-21	40	80	SLP-50+	48	70
Dist. Amp.	ISC-C3-19	10	20	SLP-10.7+	11	19
Dist. Amp.	ISC-C3-8	199	398	SLP-250+	225	320
Dist. Amp.	ISC-C3-6	6.25	12.5	SLP-10.7+	11	19
Dist. Amp.	ISC-C3-4	3.125	6.25	SLP-5+	5	8
Dist. Amp.	ISC-C3-1	42.1875	84.375	SLP-50+	48	70
Dist. Amp.	ISC-C4-26	9.0625	18.125	SLP-10.7+	11	19
Dist. Amp.	ISC-C4-22	18.125	36.25	SLP-21.4+	22	32
Dist. Amp.	ISC-C4-21	27.25	54.5	SLP-30+	32	47
Dist. Amp.	ISC-C4-20	36.25	72.5	SLP-50+	48	70
Dist. Amp.	ISC-C4-19	45.3125	90.625	SLP-50+	48	70
Dist. Amp.	ISC-C4-18	90.625	181.25	SLP-100+	98	146
Dist. Amp.	ISC-C4-17	136.25	272.5	SLP-150+	140	210
Dist. Amp.	ISC-C4-12	24.0625	48.125	SLP-30+	32	47
Dist. Amp.	ISC-C4-9	70.9375	141.875	SLP-90+	81	121
Dist. Amp.	ISC-C4-3	72.5	145	SLP-90+	81	121
Dist. Amp.	ISC-C4-1	118.125	236.25	SLP-150+	140	210
Dist. Amp.	ISC-C3-32	21.5	43	SLP-21.4+	22	32
Dist. Amp.	ISC-C3-29	35.5	71	SLP-50+	48	70
Dist. Amp.	ISC-C3-25	80	160	SLP-90+	81	121
Dist. Amp.	ISC-C4-28	9.1023	18.20	SLP-10.7+	11	19
Dist. Amp.	ISC-C4-14	24.07836	48.15672	SLP-30+	32	47
Dist. Amp.	ISC-C4-11	71	142	SLP-90+	81	121
Oscillator	ISC-C3-32	21.5	43	SLP-21.4+	22	32
Oscillator	ISC-C3-29	35.5	71	SLP-50+	48	70
Oscillator	ISC-C3-25	80	160	SLP-90+	81	121
Oscillator	ISC-C4-28	9.10023	18.20	SLP-10.7+	11	19
Oscillator	ISC-C4-14	24.07836	48.16	SLP-30+	32	47
Oscillator	ISC-C4-11	71	142	SLP-90+	81	121

Notice that every carrier frequency falls before the passband cutoff, ensuring that the carrier is not attenuated. Likewise, almost every first harmonic (the harmonic requiring the greatest attenuation) falls after the -40 dB cutoff. Those few that do not fall after the -20 dB cutoff.



I am currently completing all of the paperwork necessary to obtain approval to install the filters listed in Table 5. Once the appropriate approvals have been obtained, installation will occur during LHO's weekly four-hour maintenance periods, typically held on Tuesdays between 8:00 am and 12:00 pm PDT.

## Cable Noise Study

Another class of noise within the RF Distribution System is known as cable noise. Long stretches of RF-carrying cable have the ability to leak radio frequencies in and out if insufficiently shielded. When an RF signal leaks into a cable, the cable's primary carrier frequency cohabitates with unintended frequencies, threatening the performance of LHO's control system. Likewise, if a cable is leaking its carrier frequency into the environment, it poses a threat to any insufficiently-shielded cable in its vicinity. Therefore, it is important that physicists and engineers working at LHO fully understand the nature of cable noise and quantify the levels of cable noise currently present within the system.

My current work on understanding cable noise can be divided into two main activities. The first consists of a series of table-top experiments which seek to develop a working description of the ability of LHO's cable to transmit and receive RF signals. The second focuses on collecting the cable noise profiles of the RF transmission lines traveling from the CER to the LVEA, both for the ISC and PSL systems. Each of these activities is described in detail below.

### Cable Noise Table-Top Experiments

Often a weakly shielded RF cable receives a noise signal at one point along its path, only to transmit that signal to another cable or RF-sensitive component at another point. Because of this possibility, it is necessary to develop a thorough empirical description of the transfer of noise along a cable length. My first investigations focused on whether the output strength of a cable noise signal traveling between two pre-defined points depends upon the input power, the input frequency, or both. To answer this question, I first constructed a simple experimental apparatus, as depicted in Figure 6. At one end, the test cable receives a 10.000000 MHz input from an RF Oscillator Source. This input provides the cable with a carrier frequency, that is, the RF signal that the cable is designed to carry from the oscillator to some component connected to the RF distribution system. At the other end, the cable is terminated with  $50 \Omega$ , simulating the load provided by the component to which the RF signal is traveling. Near the input and the output, I placed ferrite chokes around the outside of the cable. By passing a second wire through each choke, I converted them into 1:1 RF power transformers. The transformers allowed me to pass an RF signal to the outside of the test cable via electromagnetic induction. Likewise, they allowed me to pass any RF signals traveling along the side of the cable to a spectrum analyzer for detailed analysis. Thus, I was able to provide an input noise signal and measure its strength and characteristics after traveling the length of the cable.

After constructing my apparatus, I first considered the effect of the input power of the noise injection on the noise output. Figure 7 shows the output power vs. the injection power for three different injection frequencies. Notice the linear trend of each series (also shown in Figure 7), which indicates that the output power is proportional to the injection power. Also notice that each linear trend has the same slope, indicating that the input frequency changes the absolute output power, but not the overall behavior of the transfer function. This observation is especially apparent in Figure 8, which depicts the loss (in dBm) of noise signal strength across an array of injection powers. Notice that the loss remains almost constant for any one injection frequency. However, it varies widely between injection frequencies.

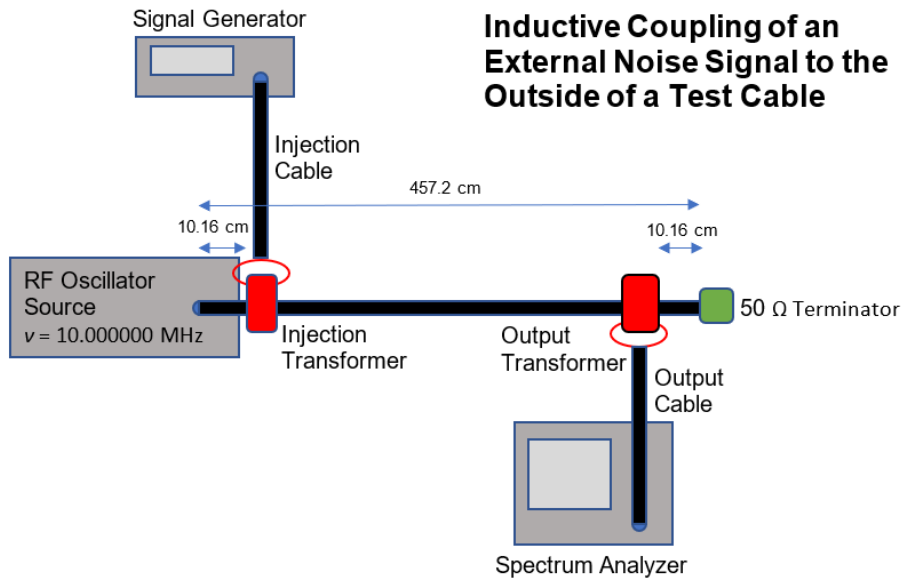


Figure 6: A diagram of my experimental apparatus, which allows me to inject RF noise on to the exterior of a cable and to measure the level of externally transmitted noise at another point along the cable.

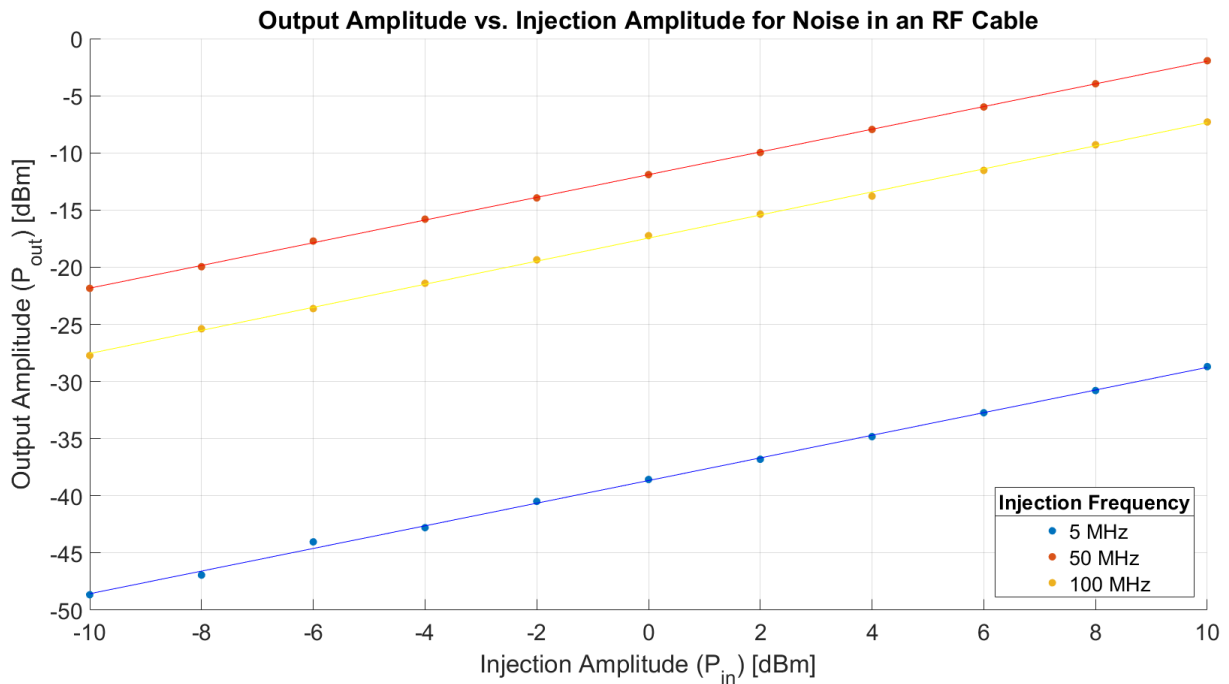


Figure 7: A plot of the output amplitude of three different noise signals across several injection amplitudes. Notice that the slope of the fitted trend lines remains constant regardless of the injection frequency.

I next considered the effect of varying the frequency of the noise injection on the power of the output noise. Figure 9 depicts this relationship for three different injection powers. Notice

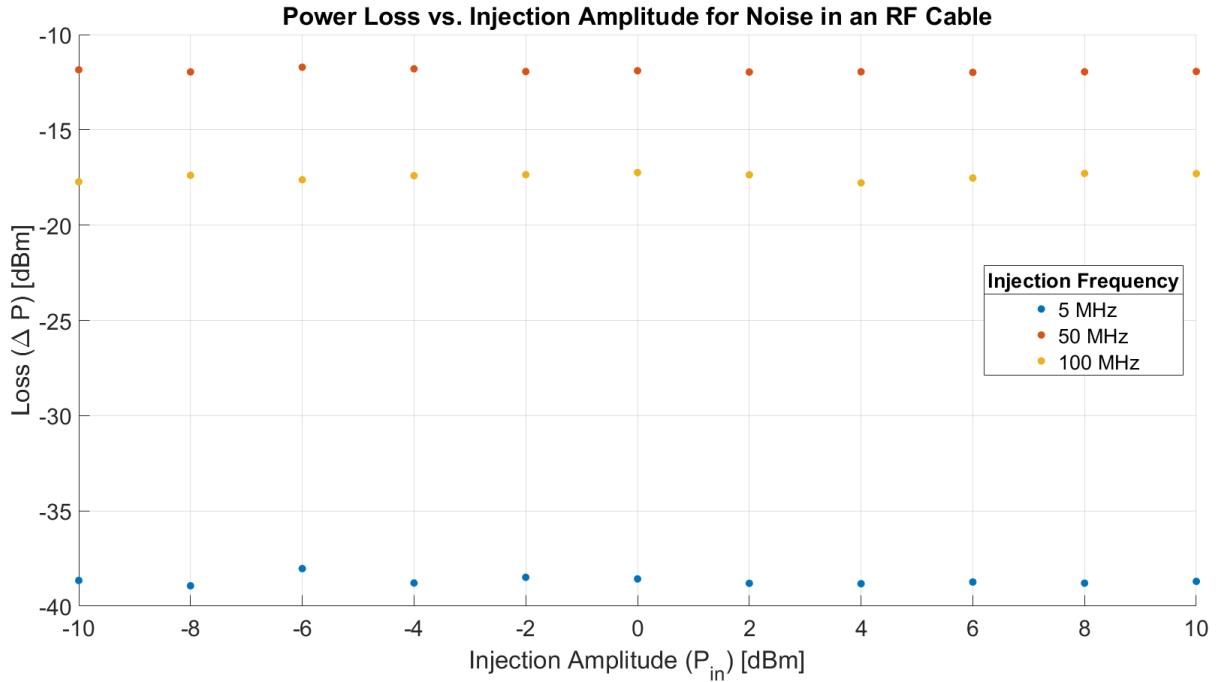


Figure 8: A plot of the power lost between a cable noise injection point and an output point across several input powers. Notice that the loss is consistent for each input frequency.

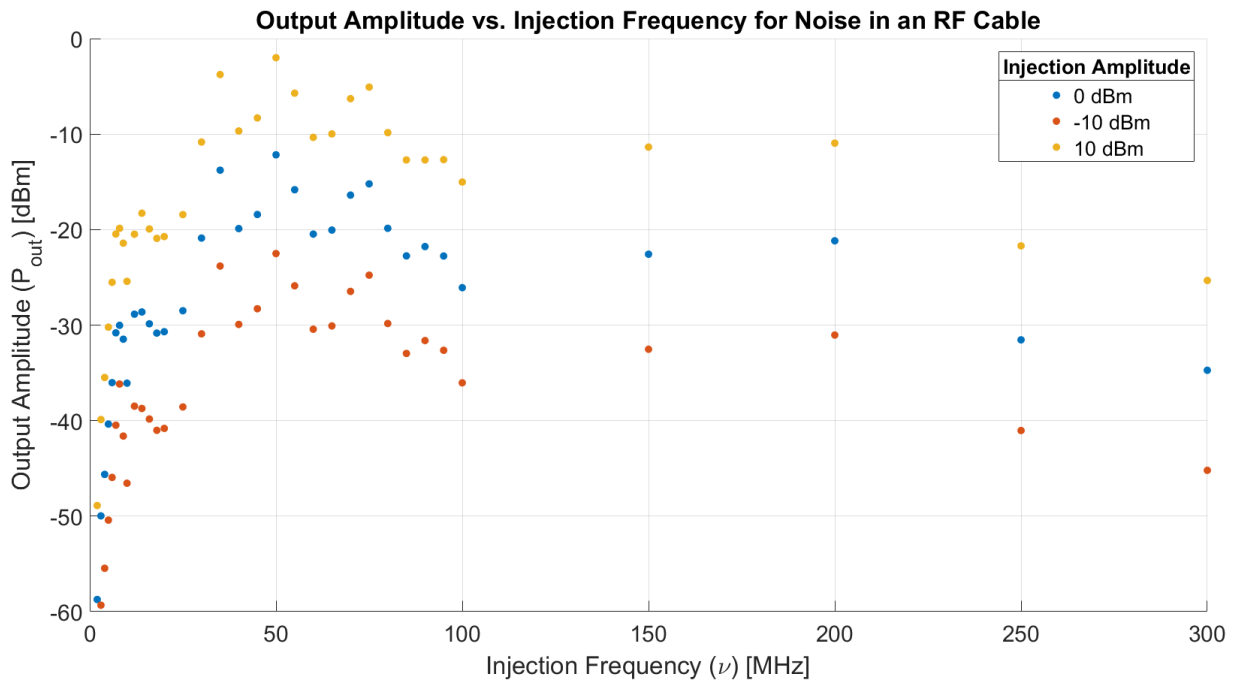


Figure 9: A plot of the output amplitude of three different noise signals across several frequencies. Notice that while the injection amplitude determines the vertical displacement of the data, the frequency dependence of the output behaves consistently.

that each input power series follows the same general trend: the output power rapidly increases

to a maximum at around 50 MHz before slowly decreasing over higher frequencies.

In summary, my work has thus far shown that the output power of a noise signal that has been injected into a cable varies linearly with respect to injection power. Furthermore, with respect to injection frequency, the output follows a rather peculiar pattern: increasing rapidly below 50 MHz and falling off slowly above that point. These observations beg several questions which I will study in my future work. First, what determines the frequency at which the output power maximizes? Second, is there a relationship between that maximum point and the carrier frequency within the cable? Finally, is the output power the same at every point along the cable, or does it depend upon the distance between the injection point and the output reading point?

### Cable Noise Profile Collection

The second half of my work on cable noise reduction has focused on creating a database of the the strongest cable noise frequencies currently plaguing the RF distribution system. To find these frequencies, I placed a choke transformer around RF cables and observed their noise signatures on a spectrum analyzer, noting the four or five largest noise lines for each. While data collection is still ongoing, Figure 10 shows the number of occurrences for several common noise lines. From this data, we quickly see that several noise lines (e.g., the 45.5 and 70.9 MHz

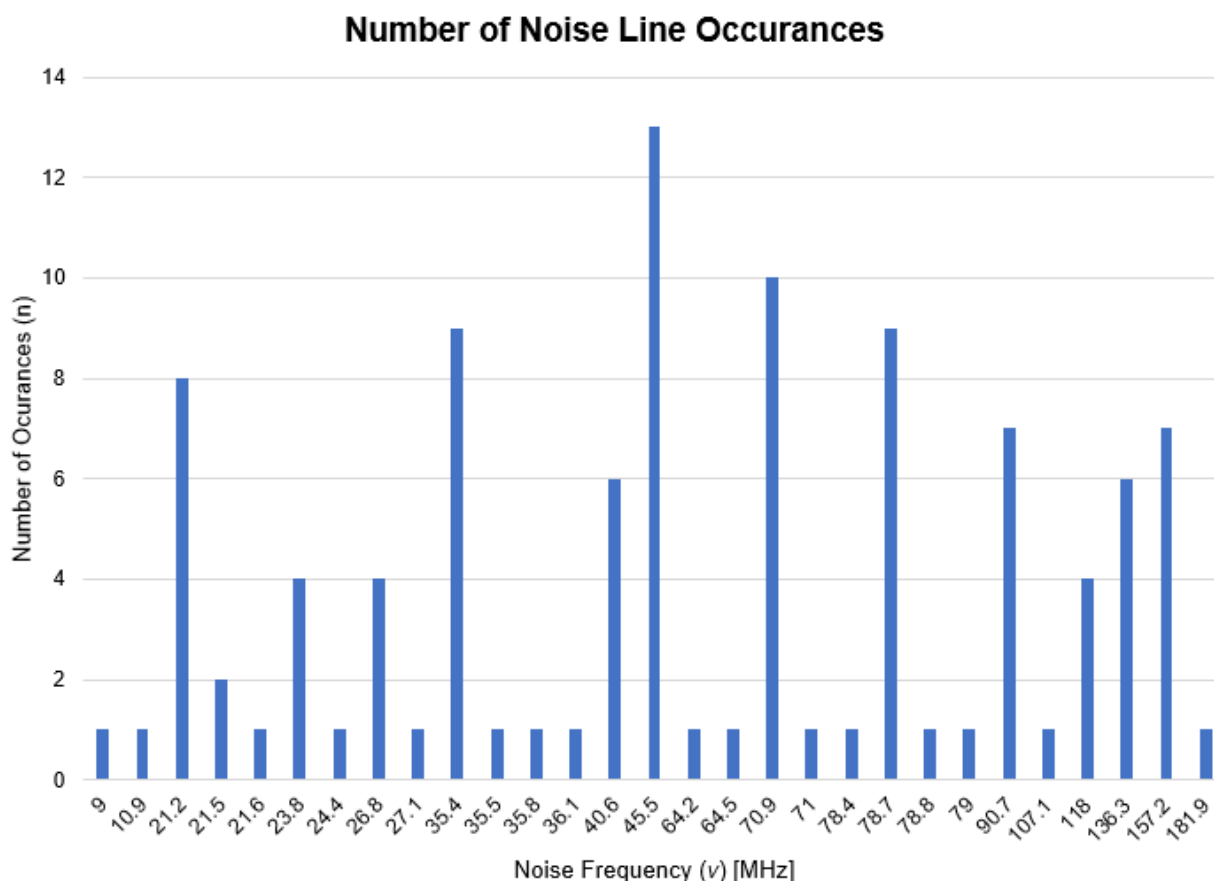


Figure 10: The prevalence of several RF noise lines within LHO’s RF distribution system.

lines) appear many times, making them prime candidates for further investigation. Once more data has been collected, I also intend to sort noise lines by IFO system (e.g., ISC and PSL) and

cable carrier frequency. These maps will help to narrow down the sources of these noise signals.

## References

[1] <http://www.wenzel.com/model/broadband-amplifier-lnba/>